Solid-State Dynamics in the closo-Carboranes

THE JOURNAL OF PHYSICAL CHEMISTRY B

Article

pubs.acs.org/JPCB

Solid-State Dynamics in the *closo*-Carboranes: A ^{11}B MAS NMR and Molecular Dynamics Study

Hernán Ahumada,[†,‡] Teresa Kurkiewicz,[†,§] Michael J. Thrippleton,[†,∥] and Stephen Wimperis*[,†]

[†]School of Chemistry and WestCHEM, University of Glasgow, Glasgow G12 8QQ, United Kingdom

[‡]Departamento de Ciencias Básicas, Universidad del Bio-Bio, Casilla 447, Chillán, Chile

[§]Department of Painting Technologies and Techniques, Nicolaus Copernicus University, Toruń, Poland

[∥]Centre for Clinical Brain Sciences, University of Edinburgh, Edinburgh EH16 4SB, United Kingdom

ABSTRACT: This work explores the dynamic behavior of the three *closo*-carborane isomers (formula $C_2B_{10}H_{12}$) using modern solid-state magic angle spinning (MAS) NMR techniques and relates the experimental measurements to theoretical results obtained using molecular dynamics simulations. At high temperatures and at B_0 = 9.4 T, the ^{11}B MAS line widths are narrow (40−90 Hz) for the three isomers. The rotational correlation times (τ_c) calculated by molecular dynamics are on the picosecond time scale, showing a quasi-isotropic rotation at these temperatures, typical for liquid systems. For all three isomers, the values of the ^{11}B spin−lattice relaxation times (T_1) show discontinuities as the temperature is decreased, confirming the phase changes reported in the literature. At low temperatures, the ^{11}B MAS spectra of all three isomers exhibit much broader lines. The simulations showed that the molecular reorientation was anisotropic around different symmetry axes for each isomer, and this was supported by the values of the reduced quadrupolar parameter P_Q^{eff} derived from "dynamic shift" measurements using ^{11}B MQMAS NMR spectroscopy. The behavior of P_Q^{eff} as a function of temperature for *p*-carborane suggests that molecular reorientation is about the C_5 symmetry axis of the molecule at low temperatures, and this was supported by the molecular dynamics simulations.

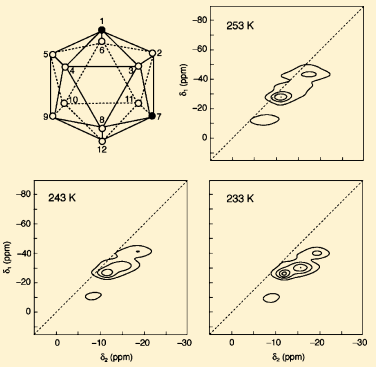

1. INTRODUCTION

The *closo*-carborane molecules ($C_2B_{10}H_{12}$) approximate regular icosahedra of CH and BH units. They exist as three structural isomers, with the carbon atoms in *o*-, *m*-, and *p*-carborane separated by one, two, and three chemical bonds, respectively.[1] As well as having similar molecular structures, the *closo*-carboranes exhibit similar motional and phase behavior in the solid state. The highest temperature solid phase occurs above 274 K for *o*-carborane, 277 K for *m*-carborane, and 303 K for *p*-carborane. X-ray diffraction studies of *o*- and *m*-carborane reveal a face-centered cubic lattice for this phase (for *o*-carborane, an additional but closely related tetragonal phase has been reported by some authors to exist between 274 and 295 K).[2−8] This is a plastic-crystalline phase, in which the near-spherical molecules reorient rapidly, yielding liquid-like NMR spectra. Below this phase boundary, the symmetry of the lattice is reduced, probably to orthorhombic symmetry for *o*- and *m*-carborane (note that the symmetries of the *p*-carborane phases have not been determined). Rapid molecular reorientation continues but is thought to be anisotropic with reorientation about at least one axis slowing significantly. At even lower temperatures (below 167 K for *o*-carborane, 165 K for *m*-carborane, and 240 K for *p*-carborane) less well characterized phases exist, in which the molecular motion is significantly reduced. Following the literature, we refer to the high-, medium-, and low-temperature solid phases for each isomer as phases I, II, and III, respectively. A summary of these phases can be found in Figure 1. It should be noted that there is no agreement in the literature on the exact phase-transition temperatures (and even, as we have mentioned above, on how many phases occur and what their symmetries are); here we have followed Leites[6] and Winterlich et al.[8] for the transition temperatures.

Although a number of NMR studies exist in the literature,[2−5,8] many of these are more than 20 years old and therefore do not exploit modern NMR methods, such as magic angle spinning (MAS) and multiple-quantum MAS (MQMAS).[9] In this paper, we show that modern ^{11}B MAS NMR techniques provide a window on the structure and dynamics of the *closo*-carboranes. In particular, we show that molecular reorientation can be easily and semiquantitatively probed by measurement of the ^{11}B (spin I = 3/2) motionally averaged second-order quadrupolar isotropic shift, known as the "dynamic shift" in liquid-state NMR studies.[10−13]

To support our experimental results, we have performed several molecular dynamics simulations in the temperature range where the NMR experiments were recorded. In the literature, we can find only one previous molecular dynamics simulation for a *closo*-carborane system. This work dates from 1996, with only 35 ps of trajectory calculated, and does not

Received: January 3, 2015
Revised: February 23, 2015
Published: February 24, 2015

DOI: 10.1021/acs.jpcb.5b00043
J. Phys. Chem. B 2015, 119, 4309−4320

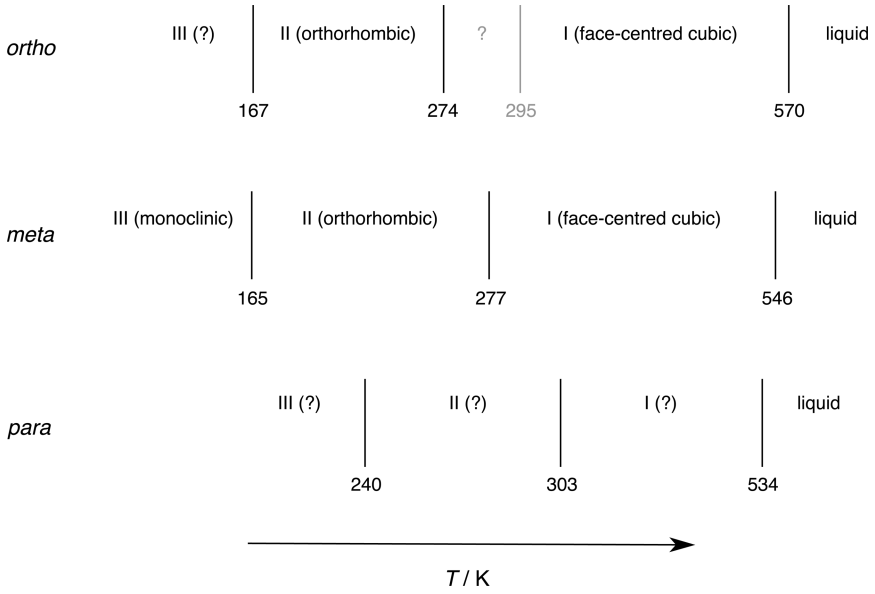

Figure 1. Schematic representation of the solid phases of the *o*-, *m*-, and *p*-isomers of carborane. The transition temperatures are taken from Leites[6] and Winterlich et al.[8]

provide the detail we need for comparison with our NMR results.[14]

2. EXPERIMENTAL DETAILS

General NMR. Experiments were performed using a Bruker Avance NMR spectrometer equipped with a wide-bore 9.4 T magnet (corresponding to ^{1}H and ^{11}B Larmor frequencies of 400.1 and 128.4 MHz, respectively) and a 4 mm MAS probehead. Chemical shifts are reported in ppm relative to $BF_3{\cdot}OEt_2$ for ^{11}B (solid BPO_4 with a ^{11}B shift of −3.3 ppm was used as a secondary reference) and TMS for ^{1}H. All experiments employed MAS at a frequency of 10 kHz, and low-temperature measurements were carried out by passing the rotor bearing gas through a liquid nitrogen-cooled heat exchanger. As a consequence of the frictional sample heating due to MAS and the resulting spatial inhomogeneity of the sample temperature, which we have estimated using ^{207}Pb MAS NMR of lead(II) nitrate, $Pb(NO_3)_2$, the temperatures quoted in this article are likely to have a precision of ±5 K and to underestimate the temperature at the center of the sample by approximately 5 K. Radio-frequency field strengths of 140−170 kHz for non-selective ^{11}B pulses (i.e., 90° pulse durations in the range 1.5−1.8 μs) and 170 kHz for ^{1}H pulses were used.

^{11}B MAS NMR. ^{1}H-decoupled ^{11}B MAS NMR spectra of three isomers of carborane were recorded as a function of temperature in the range 223−293 K for *o*- and *m*-carborane and in the range 223−333 K for *p*-carborane. ^{1}H decoupling was applied with a field strength of 50 kHz. The recycle interval (in the range 1−4 s) was optimized to ensure that the samples returned to equilibrium prior to excitation, and spectra are the result of averaging eight transients.

^{11}B MQMAS. Variable-temperature ^{1}H-decoupled ^{11}B MQMAS NMR spectra of *o*-, *m*-, and *p*-carborane were obtained using the method described in Figure 1a of ref 15; the three-pulse "sandwich" was found to be most generally effective for excitation of triple-quantum coherence because of the small magnitude of the residual quadrupolar splittings. ^{1}H decoupling was used, with a field strength of 50 kHz. The triple-quantum excitation period, τ_{ex}, was optimized for each temperature and isomer in the range 10−40 μs; a *z*-filter interval of 5 μs was employed. The States−Haberkorn−Ruben method of δ_1 sign discrimination was used, and pure-absorption two-dimensional line shapes by means of a hypercomplex Fourier transform were obtained. Twenty-four transients were averaged for each of 30−38 (*o*-carborane), 30−57 (*m*-carborane), and 60−67 (*p*-carborane) t_1 values, with a t_1 increment of 50 μs. The ^{11}B MQMAS NMR spectrum of *p*-carborane recorded at 223 K was obtained using the same pulse sequence, but on account of the larger residual quadrupolar splittings in this case, triple-quantum coherence was excited with a single pulse (as normally used in MQMAS) instead of the three-pulse sandwich. All pulses used were nonselective (because of the generally small residual quadrupolar splittings). Twenty-four transients were averaged for each of 32 t_1 values, with a t_1 increment of 25 μs.

Double-INEPT. In phase I, ^{11}B triple-quantum coherences could not be excited by conventional means; hence, triple-quantum (^{11}B)−single-quantum (^{1}H) MAS correlation spectra were recorded using the "double-INEPT" technique described in Figure 1b of ref 15, which utilizes the ^{1}H−^{11}B *J*-coupling to excite ^{11}B triple-quantum coherences. ^{11}B decoupling was applied during acquisition, with a radio-frequency field strength of 55 kHz. A coherence transfer interval τ of 2 ms and recycle intervals in the range 1−2 s were used. 48 transients were averaged for each of 64−80 t_1 values, with a t_1 increment of 50 or 100 μs.

T_1 Measurement. ^{11}B spin−lattice relaxation times (T_1) were measured using the inversion−recovery experiment. As elsewhere in this work, nonselective ^{11}B excitation was assumed on account of the generally small residual quadrupolar splittings, and the amplitude of the ^{11}B MAS centerband was used in the determination of T_1. The inversion−recovery intervals used were optimized for each temperature and isomer, within a range of 3 μs−5 s.

Molecular Dynamics Simulations. The system consisted of a box of initial size 4.0 nm × 3.5 nm × 4.5 nm, with 216 molecules per box. The size of this box evolves in the course of a molecular dynamics simulation in response to structural

DOI: 10.1021/acs.jpcb.5b00043
J. Phys. Chem. B 2015, 119, 4309−4320

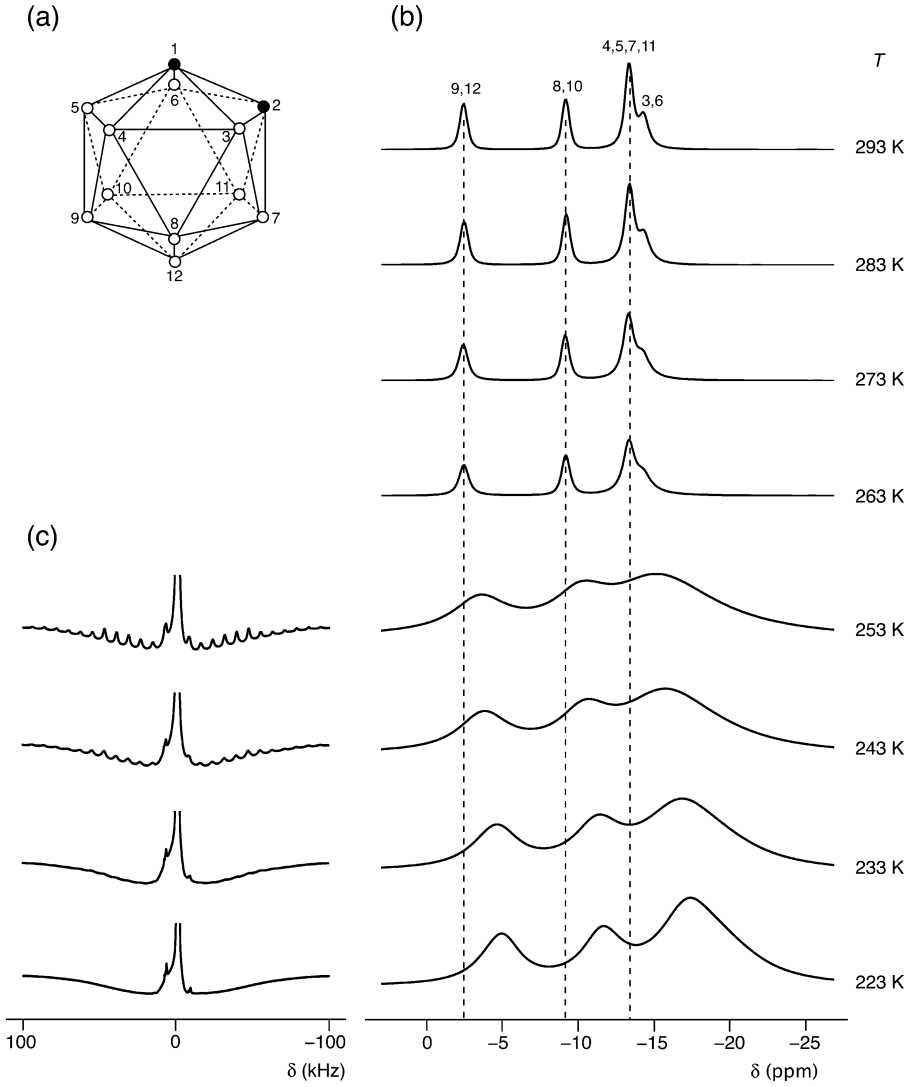

Figure 2. (a) Chemical structure of *o*-carborane. The boron (white circles) and carbon atoms (black circles) form an icosahedron; hydrogen atoms have been omitted for clarity. (b) Variable-temperature ^{1}H-decoupled ^{11}B MAS NMR spectra of *o*-carborane. (c) ^{1}H-decoupled ^{11}B MAS NMR spectra of the low-temperature phase (phase II) of *o*-carborane with a wide spectral width, showing the spinning sidebands. The numbering above the peaks in (b) corresponds to that of the boron atoms in (a).

changes. Eight simulations were performed between 280 and 350 K for *o*- and *m*-carborane and six simulations for *p*-carborane between 310 and 360 K. Trajectories of 200 ns were calculated at 280 and 290 K, 100 ns at 300 and 310 K, and 50 ns at other temperatures. In addition, simulated annealing trajectories of 100 ns were calculated from 150 to 350 K for each isomer. (Note that the theoretical temperatures used in the molecular dynamics simulations, which are derived from the total kinetic energy of the system, are not true statistical temperatures and are not expected to agree with the experimental temperatures measured here and in previous work.) Calculation of all trajectories and subsequent analyses were performed using the software package Gromacs v. 4.5.3.[16] The Visual Molecular Dynamics (VMD) program was employed for trajectory visualization and graphics.[17] A 1.4 nm cutoff was used for the Lennard-Jones potentials, and 1 nm was used for real-space electrostatic potentials. Long-range electrostatic interactions were calculated using the particle mesh Ewald (PME) algorithm.[18−20] The neighbor list was updated every 10 time steps. Temperature and pressure (1 bar) were kept constant, using a weak coupling algorithm[21] with time constants 0.1 and 1.0 ps, respectively. All trajectories were calculated with a time step size of 2 fs. The Lennard-Jones parameters for boron, carbon, and hydrogen were the same as those used by Gamba et al.[14] The bonding interactions were calculated using the force field developed by Allinger and co-workers.[22]

3. RESULTS AND DISCUSSION

Molecular Motion and the Second-Order Quadrupolar Interaction. The coupling between the nuclear quadrupole moment and the molecular electric field gradient is an anisotropic interaction of spatial rank two, normally parametrized by a coupling constant C_Q and an asymmetry η. In high-field NMR, this quadrupolar interaction can be treated using average Hamiltonian theory, yielding the well-known first- and second-order quadrupolar interactions, which have spatial ranks two and zero, two and four, respectively. Since the average Hamiltonian is obtained by averaging over the Larmor period, the effect of dynamics on the second-order quadrupolar interaction depends on the time scale of any molecular motion

DOI: 10.1021/acs.jpcb.5b00043
J. Phys. Chem. B 2015, 119, 4309−4320

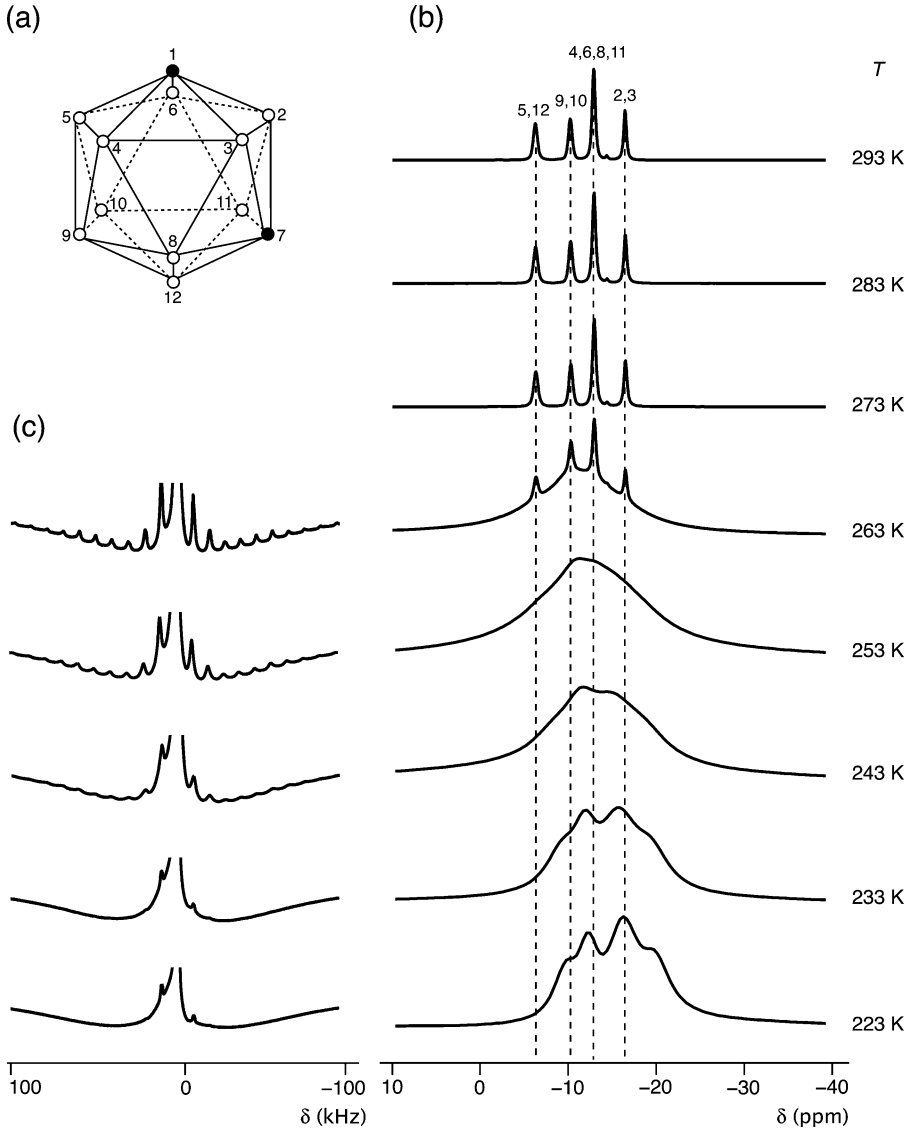

Figure 3. (a) Chemical structure of *m*-carborane. The boron (white circles) and carbon atoms (black circles) form an icosahedron; hydrogen atoms have been omitted for clarity. (b) Variable-temperature ^{1}H-decoupled ^{11}B MAS NMR spectra of *m*-carborane. (c) ^{1}H-decoupled ^{11}B MAS NMR spectra of the low-temperature phase (phase II) of *m*-carborane with a wide spectral width, showing the spinning sidebands. The numbering above the peaks in (b) corresponds to that of the boron atoms in (a).

compared with the Larmor period. For motion that is much slower than the Larmor frequency ν_0, the average Hamiltonian expansion remains valid, and the spectrum can be determined by calculating the time-averaged second-order Hamiltonian. Thus, if the motional rate constant is significantly larger than the second-order quadrupolar parameter C_Q^2/ν_0 (but still much smaller than ν_0), the second- and fourth-rank terms are averaged and, in the case of isotropic motion, are reduced to zero. The zeroth-rank term, however, is orientation independent and unaffected by motion on this time scale; the isotropic quadrupolar shift is therefore unaffected. In the opposite case, where motion is much faster than the Larmor precession, the effect of orientational averaging must be assessed *before* the average Hamiltonian is calculated. This means that both the second-order broadening and the isotropic quadrupolar shift are affected, and since the full quadrupolar Hamiltonian is second rank, rapid isotropic motion averages both to zero. Molecular motion on the nanosecond time scale or faster—in both solids and liquids—can therefore have a measurable influence on the center-of-gravity shifts of quadrupolar nuclei. This effect has been extensively studied in solution, where it is commonly referred to as the dynamic shift.[10−13] As pointed out by Werbelow and London, however, it is better described as a quenching of the isotropic second-order quadrupolar shift by rapid reorientational motion.[13]

^{11}B MAS NMR Spectra of *o*-Carborane, *m*-Carborane, and *p*-Carborane: Centerbands. Figures 2, 3, and 4 show ^{11}B MAS spectra of the three carborane isomers, respectively, recorded as a function of temperature. As noted by Harris et al., at higher temperature the spectra are remarkable for their narrow line widths (*o*-carborane: 80−90 Hz; *m*-carborane: 70−80 Hz; *p*-carborane: 40 Hz).[4] ^{11}B MAS central-transition line widths in the solid state are typically on the order of kilohertz owing to the quadrupolar coupling and other broadening interactions. The high-temperature carborane spectra resemble liquid-state NMR spectra and are thus consistent with the assumption of molecules undergoing rapid isotropic reorientation. Furthermore, the spectra change very little with cooling

DOI: 10.1021/acs.jpcb.5b00043
J. Phys. Chem. B 2015, 119, 4309−4320

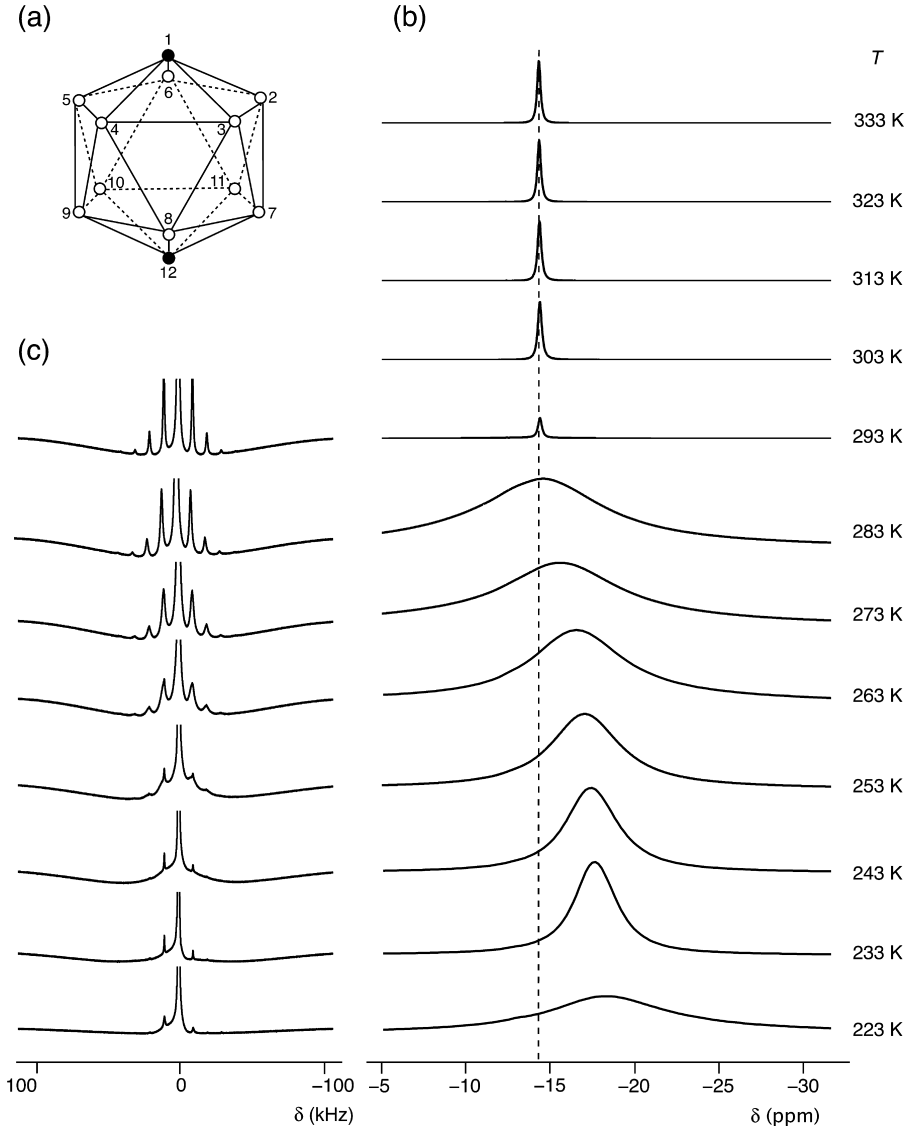

Figure 4. (a) Chemical structure of *p*-carborane. The boron (white circles) and carbon atoms (black circles) form an icosahedron; hydrogen atoms have been omitted for clarity. (b) Variable-temperature ^{1}H-decoupled ^{11}B MAS NMR spectra of *p*-carborane. (c) ^{1}H-decoupled ^{11}B MAS NMR spectra of the low-temperature phases (phases II and III) of *p*-carborane with a wide spectral width, showing the spinning sidebands.

until the I−II phase transition is reached, suggesting motional rate constants that are orders of magnitude greater than the size of the quadrupolar coupling constant (typically on the order of 1 MHz) and the Larmor frequency (128.4 MHz) across the temperature range. As a result of the narrow lines, the number of peaks observed is equal to the number of unique boron chemical environments for each isomer, and the peaks have been assigned by comparison with solution-state NMR data[4] and quantum chemical calculations.[23]

Below the I−II phase transition, the spectra of all three isomers exhibit significantly broader lines (*o*-carborane: 600 Hz; *m*-carborane: 500−1000 Hz; *p*-carborane: ∼1200 Hz). This is consistent with the transition to a more solid-like phase, where molecular reorientation slows significantly about at least one molecular axis, so that broadening interactions are not fully averaged. Furthermore, as the samples are cooled, the central-transition lines narrow somewhat, suggesting a rate of reorientation below the Larmor frequency. For *p*-carborane, the line width increases again at the II−III phase transition, from 400 Hz at 233 K to 1.3 kHz at 223 K.

(Decreasing) temperature also affects the frequencies of the peaks. For *o*-carborane, a shift to low frequency is observed at the I−II transition, while for *m*- and *p*-carborane the change occurs more gradually below the phase transition (a further shift to low frequency is observed for *p*-carborane at the II−III transition). As discussed below, the frequency changes are likely to be "dynamic shift" effects, rather than changes in the chemical shift, consistent with the assumption that the phase changes affect the reorientational behavior but do not significantly alter the molecular structure.

^{11}B MAS NMR Spectra of *o*-Carborane, *m*-Carborane, and *p*-Carborane: Spinning Sidebands. For all three isomers, very little spinning sideband intensity is apparent in phase I, and the few sidebands observed are likely to result from shimming imperfections or susceptibility effects. This is consistent with rapid isotropic motion, which averages out the quadrupolar interaction and causes the satellite-transition signal to be concentrated in the centerband. Many more spinning sidebands appear below the I−II phase transition temperature (Figures 2c, 3c, and 4c), spanning approximately

DOI: 10.1021/acs.jpcb.5b00043
J. Phys. Chem. B 2015, 119, 4309−4320

300 kHz for *o*- and *m*-carborane and 80 kHz for *p*-carborane, consistent with more anisotropic motion that results in incomplete averaging of the quadrupolar interaction. It is interesting to note that the spinning sideband pattern for *p*-carborane is significantly narrower than for the other two isomers. This observation is consistent with rapid anisotropic reorientation about the C_5 symmetry axis, which would average the quadrupolar coupling constant to a small fraction of its intrinsic value (see below); alternatively, the reorientation may simply be more isotropic in the *p*-carborane isomer.

A further point to note is that the widths of the spinning sidebands increase as the temperature is reduced, until they disappear into the baseline. This is likely to be the result of motional broadening, which causes the sideband line width to increase as the rate of reorientation approaches the size of the quadrupolar coupling interaction.[24,25] This implies that molecular reorientation remains faster than ∼1 MHz immediately below the I−II phase transition.

Longitudinal Relaxation. The T_1 discontinuities seen in Figure 5 confirm the phase changes inferred from the MAS spectra. As the temperature is reduced in phase I, T_1 decreases, suggesting that the reorientation rate constant exceeds the ^{11}B Larmor frequency (128.4 MHz). Below the I−II phase transition, longitudinal relaxation is more rapid, and T_1 increases as the temperature is reduced, implying molecular reorientation with a rate constant below the Larmor frequency. Phase III of *p*-carborane has a much longer T_1 than the higher temperature phases, consistent with significantly retarded reorientation.

Multiple-Quantum NMR and Dynamic Shift Measurement. Figures 6, 7, and 8 show variable-temperature ^{11}B MQMAS spectra of the three unsubstituted carboranes. As well as increasing the effective resolution compared with the one-dimensional MAS spectra, MQMAS permits the measurement of dynamic shift effects. This is possible because chemical shifts appear with a 1:3 ratio in the single- and triple-quantum dimensions of the spectrum, while quadrupolar shifts appear in a −1:3 ratio (for spin I = 3/2 nuclei). Peaks with no quadrupolar shift are therefore centered on the line $\delta_1 = 3 \times \delta_2$, while peaks with a quadrupolar shift are displaced "below" this line.

It is evident from the MQMAS spectra that the peaks exhibit dynamic shifts. These increase as the temperature is reduced, although the magnitude and temperature dependence vary from site to site. The extent of the quadrupolar shift depends on both the strength of the quadrupolar interaction and on any molecular motion and can be characterized by an "effective quadrupolar product" P_Q^{eff}, as described in ref 15. P_Q^{eff} ranges between zero, when rapid (faster than the Larmor frequency) isotropic motion, quenches the quadrupolar interaction, and, in the absence of motion, $P_Q = C_Q(1 + \eta^2/3)^{1/2}$. Figure 9 shows the variation of P_Q^{eff} as a function of temperature for each resolved MQMAS peak; also shown (dashed lines) are the intrinsic P_Q values predicted by *ab initio* calculation.[23]

For all of the isomers, intermediate values of P_Q^{eff}, which increase with decreasing temperature, are observed, implying that the rate of motion in phase II is of the same order of magnitude as the Larmor frequency. For *o*-carborane, the three resolved peaks yield very different P_Q^{eff} values across the temperature range, even though *ab initio* calculations suggest similar intrinsic P_Q values for all sites. The range of observed P_Q^{eff} is therefore suggestive of anisotropic reorientation. At the lowest temperature, 223 K, P_Q^{eff} for the 9,12 environment

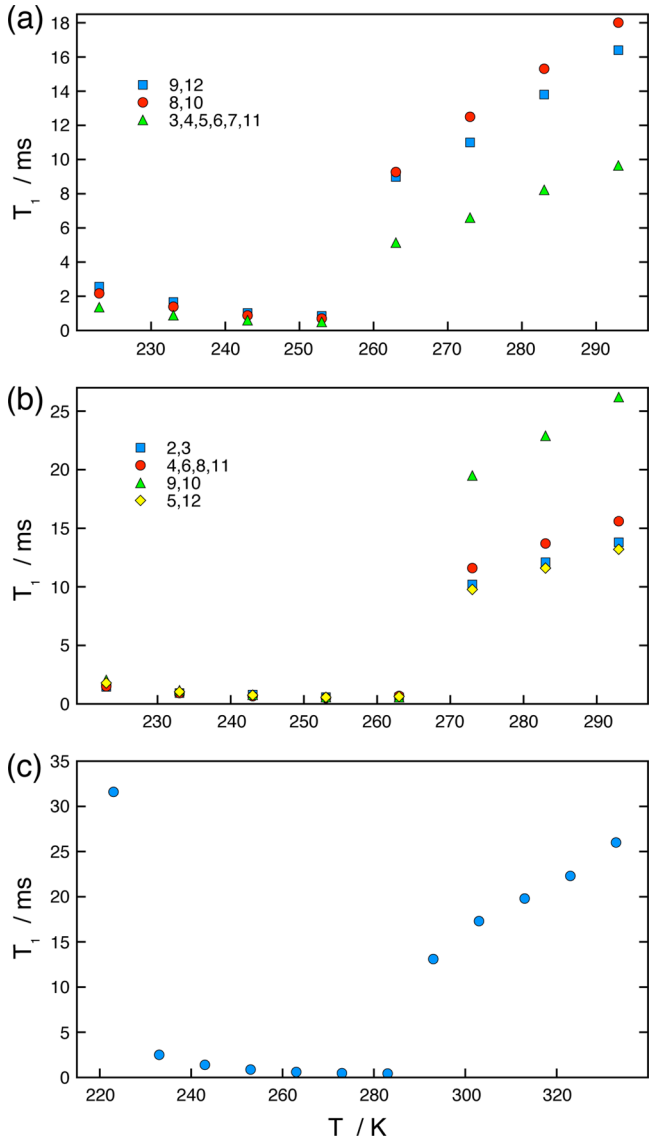

Figure 5. ^{11}B spin−lattice relaxation times (T_1) as a function of temperature (T) for the three isomers of carborane. The *o*- and *m*-isomers exhibit evidence of a qualitative change in motional behavior (equivalent to the thermodynamic phase transition) at about 260 and 270 K, respectively. The *p*-isomer shows two such phase transitions: one in the vicinity of 290 K and other in the vicinity of 230 K.

remains significantly lower than the calculated intrinsic P_Q, indicating that motion is not fully quenched at the lowest temperature observed.

For *m*-carborane, the P_Q^{eff} values remain closer together than for *o*-carborane, are near-zero at high temperature, and are closer to the calculated intrinsic P_Q values at low temperature. These observations suggest that molecular reorientation is more isotropic than for *o*-carborane at high temperatures and is slower at low temperature.

For *p*-carborane, P_Q^{eff} falls steadily toward zero as the temperature is increased. This could suggest that reorientation is fast and relatively isotropic just below the I−II phase transition, which is consistent with the suggestion of Beckman and Leffler that the absence of an electrostatic molecular dipole moment in *p*-carborane leads to reduced intermolecular interactions and less anisotropic reorientation compared with the other isomers.[2] Another possibility is that the dominant

DOI: 10.1021/acs.jpcb.5b00043
J. Phys. Chem. B 2015, 119, 4309−4320

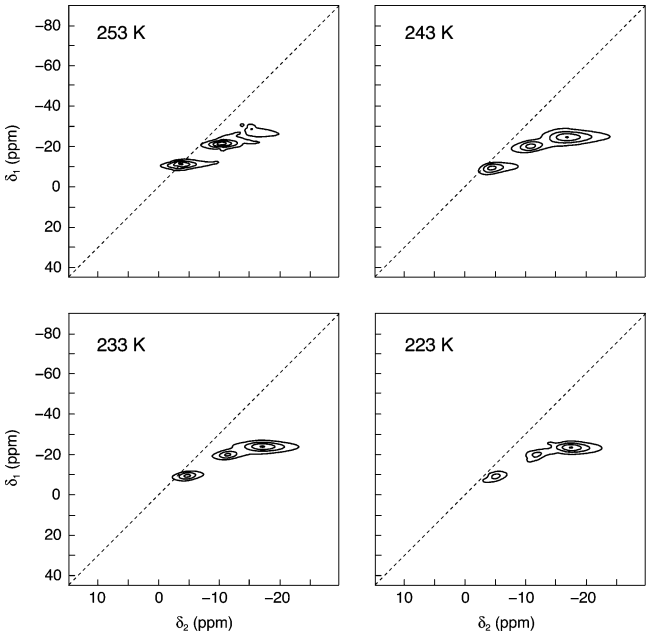

Figure 6. Variable-temperature ^{1}H-decoupled ^{11}B MQMAS NMR spectra of *o*-carborane obtained using the pulse sequence in Figure 1a of ref 15. The +3 diagonal is shown as a dotted line in each spectrum.

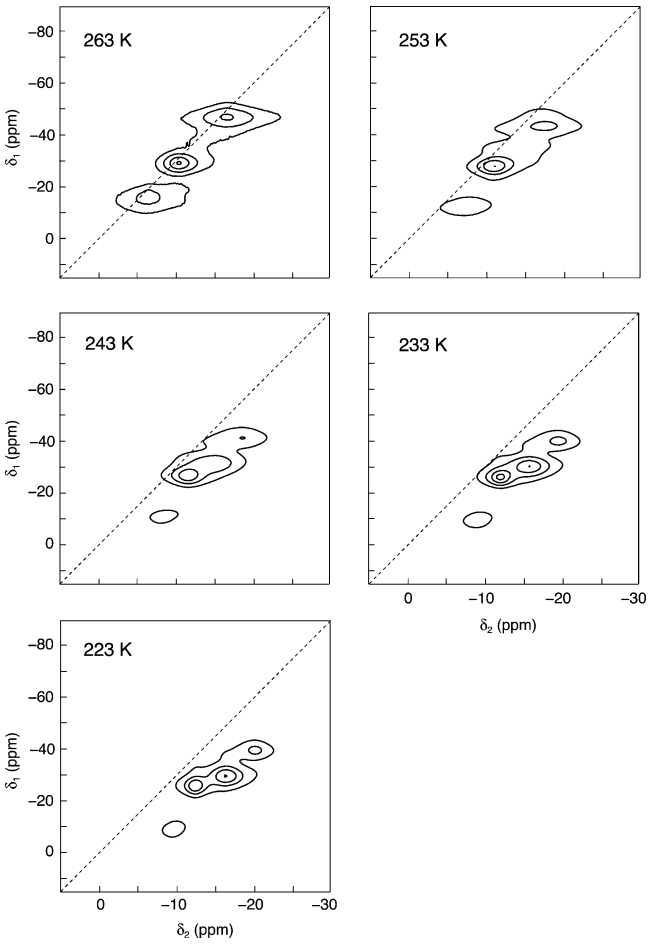

Figure 7. Variable-temperature ^{1}H-decoupled ^{11}B MQMAS NMR spectra of *m*-carborane obtained using the pulse sequence in Figure 1a of ref 15. The +3 diagonal is shown as a dotted line in each spectrum.

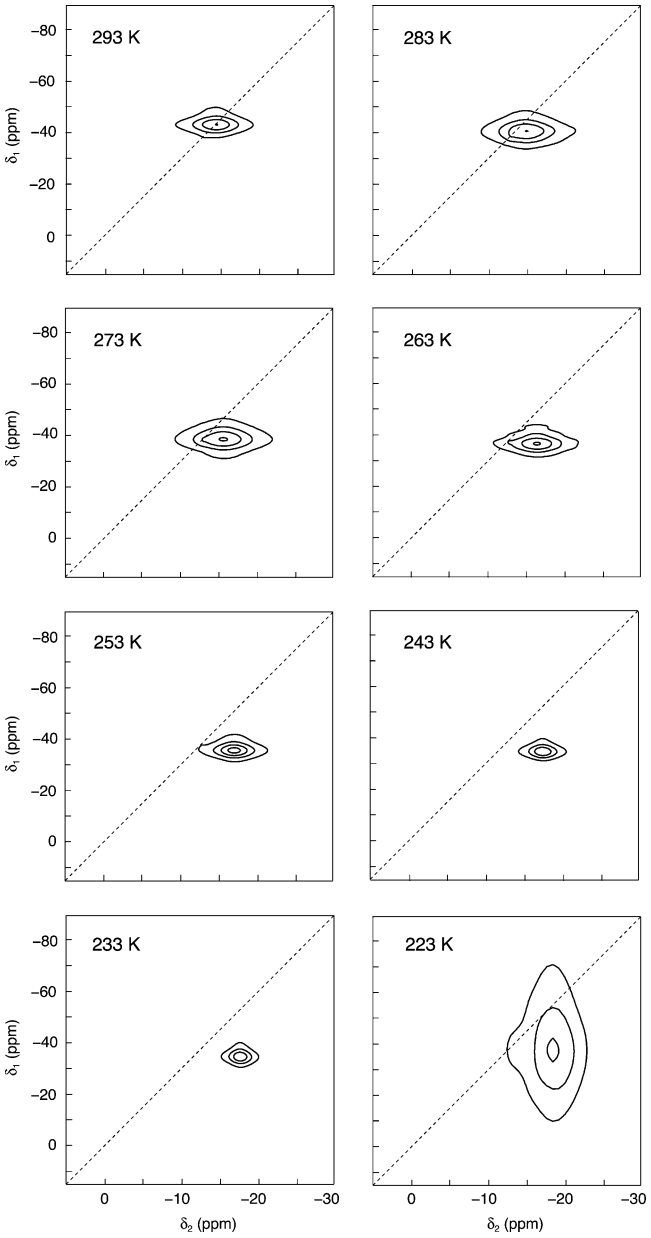

Figure 8. Variable-temperature ^{1}H-decoupled ^{11}B MQMAS NMR spectra of *p*-carborane obtained using the pulse sequence in Figure 1a of ref 15. The +3 diagonal is shown as a dotted line in each spectrum.

mode of reorientation is about the C_5 symmetry axis of the molecule; since the angle between this axis and the largest principal axis of the quadrupolar coupling tensor is close to the magic angle, rapid rotation would then average the quadrupolar shift to a small fraction of the static value. Although the lowest temperature data point at 223 K corresponds to phase III, P_Q^{eff} is close to that measured at 233 K.

For samples in the "isotropic phase" (phase I), we were unable to excite triple-quantum coherence using the MQMAS experiment. However, it was possible to excite triple-quantum coherence in this phase using the double-INEPT approach described in Figure 1b of ref 15. For each of the isomers, the triple-quantum frequency was found to be 3 times the single-quantum frequency, indicating a P_Q^{eff} of zero and implying isotropic motion at a rate faster than the Larmor frequency.

DOI: 10.1021/acs.jpcb.5b00043
J. Phys. Chem. B 2015, 119, 4309−4320

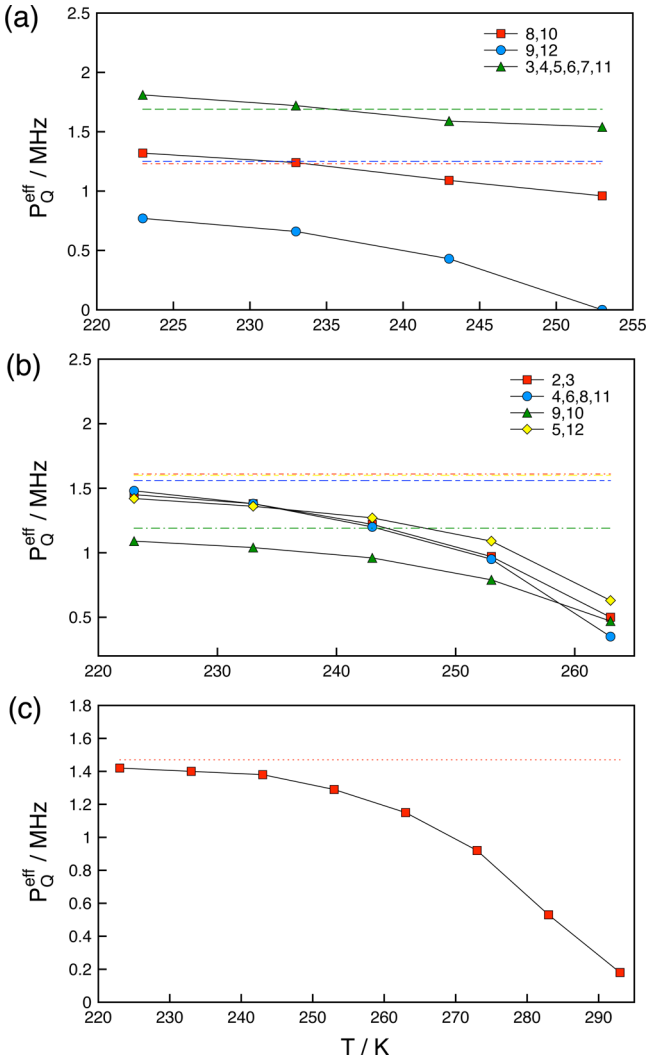

Figure 9. Variation of P_Q^{eff} with temperature for the chemically distinct ^{11}B environments in the three isomers: (a) *o*-carborane, (b) *m*-carborane, and (c) *p*-carborane. The P_Q^{eff} values were determined from the dynamic or second-order shifts in the MQMAS spectra in Figures 6, 7, and 8. The horizontal dashed lines indicate theoretical P_Q values derived from *ab initio* calculations. The assignment of the symbols in (a) and (b) refers to the numbering scheme for the boron atoms and peaks in Figures 2 and 3. Note that the peaks representing the B3/B6 and B4/B5/B7/B11 environments in *o*-carborane overlap in the low-temperature phase (phase II) and so cannot be distinguished in the MQMAS spectra.

Molecular Dynamics Simulations. Using molecular dynamics simulations, a simulated annealing run was performed for each isomer to analyze the motional behavior as a function of the temperature. Figure 10 shows the variation of the angle between a number of CH or BH bonds in one *m*-carborane molecule and the *z*-axis of the box during the course of the simulated annealing. Three different regions of motional behavior can be appreciated. One, at a high simulation temperature, above 310 K, shows the angles with respect to the *z*-axis exploring almost all possible values on a rapid time scale. This region can be described as corresponding to fast isotropic motion about three orthogonal molecular moments of inertia, which the previous experimental results have referred to as phase I. (Remember that these theoretical temperatures used in the molecular dynamics simulations are expected to agree

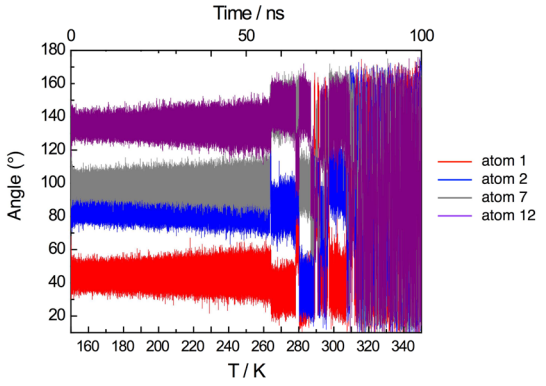

Figure 10. Variation of the angle between selected CH or BH bonds in a single *m*-carborane molecule and the *z*-axis of the molecular dynamics box during the course of a 100 ns simulated annealing run from 150 to 350 K. "Atoms" 1 and 7 correspond to a CH bond, and "atoms" 2 and 12 correspond to a BH bond (see Figure 3a).

only very approximately, if at all, with the experimental temperatures.) In the second region, between 265 and 310 K, the value of the angles fluctuate rapidly over a much smaller range, maybe ±15°, but also undergo much larger jumps on a much slower time scale. This means that there is a component of the molecular rotation that is much slower, and if the larger jumps are restricted to certain values, this slower component could be anisotropic. Therefore, this region would appear to correspond to phase II observed experimentally. The third region is found at low simulation temperature in Figure 10, below 265 K: here, the angles fluctuate rapidly over the small ±15° but are otherwise constant, suggesting that the molecule has a fixed orientation when averaged over a long time scale. This region appears to correspond to phase III in the experimental results.

To obtain more details about the structure and molecular motion in each system, we performed longer molecular dynamics simulations at several temperatures. The initial position for the simulation at each temperature was taken from the simulated annealing run performed for each isomer. Figure 11a shows the box used for each simulation. As the results in the literature suggest, a face-centered cubic unit cell can be identified inside the box for all three isomers, as shown in Figure 11b. This face-centered unit cell appears to be retained all temperatures in our molecular dynamics simulations, indicating that any deviations from cubic symmetry are smaller than the thermally driven fluctuations in the position of each molecule. Therefore, the changes in crystal symmetry indicated by the X-ray diffraction studies in the literature cannot be studied by the molecular dynamics methods used here. Nevertheless, our methods can visualize changes in structure and motional behavior.

As shown in Figure 12, the average final volume of the simulation box decreases as temperature decreases. Distinct changes in the gradients are observed at temperatures corresponding to the changes in motional behavior observed in the simulated annealing. In each case, two different motional/volume regions can be appreciated. In the cases of *m*- and *p*-carborane, there are sharp changes in volume occurring at about 315 and 345 K, respectively. In contrast, *o*-carborane shows a more gradual decrease in the volume as the simulation temperature is decreased from 320 to 300 K.

To study the temperature-related changes in the average structure of the unit cell, we have calculated the pair

DOI: 10.1021/acs.jpcb.5b00043
J. Phys. Chem. B 2015, 119, 4309−4320

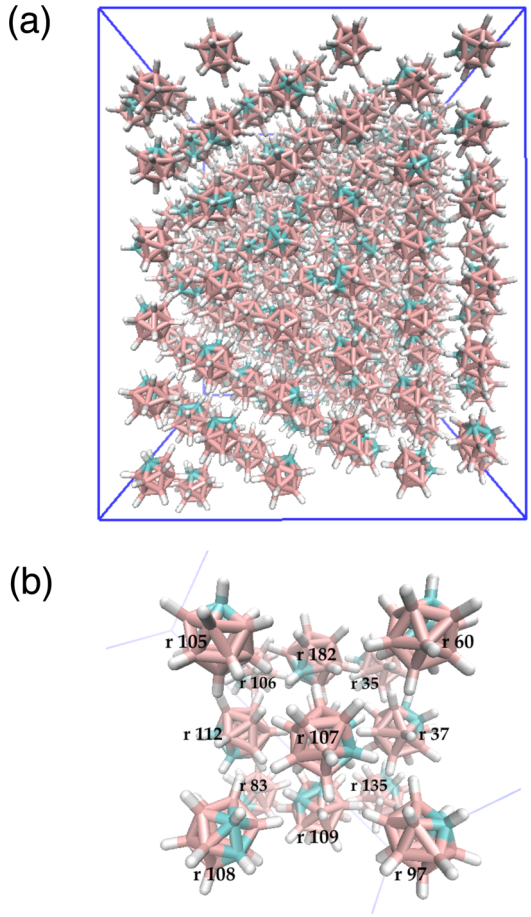

Figure 11. Snapshot of the *o*-carborane system after 30 ns of simulated annealing. (a) View of the whole molecular dynamics box with 216 molecules of *o*-carborane. (b) Face-centered cubic unit cell from near the center of the simulated system. Boron atoms are pink, carbons are cyan, and hydrogen are white.

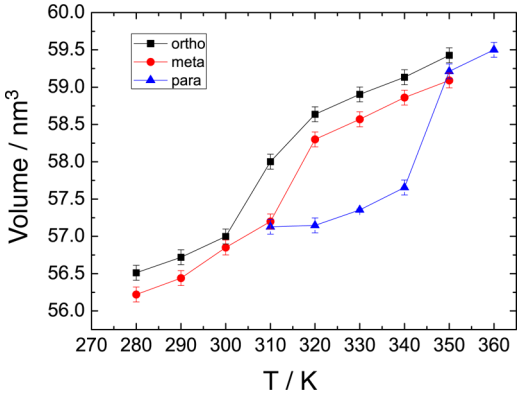

Figure 12. Average volume of the molecular dynamics box for the three carborane isomers over the course of molecular dynamics simulations run at various temperatures.

distribution function (PDF) up to a radius of 1.75 nm for each isomer. Figure 13 shows the PDF between 1.36 and 1.55 nm, corresponding to the fourth coordination sphere, for each isomer. Similar behavior is found for the other coordination spheres. As the centers of mass of the molecules are not static in the box, the instantaneous distribution of pairwise distances has a finite width. In general, as the simulation temperature decreases the width of each distribution decreases, while its

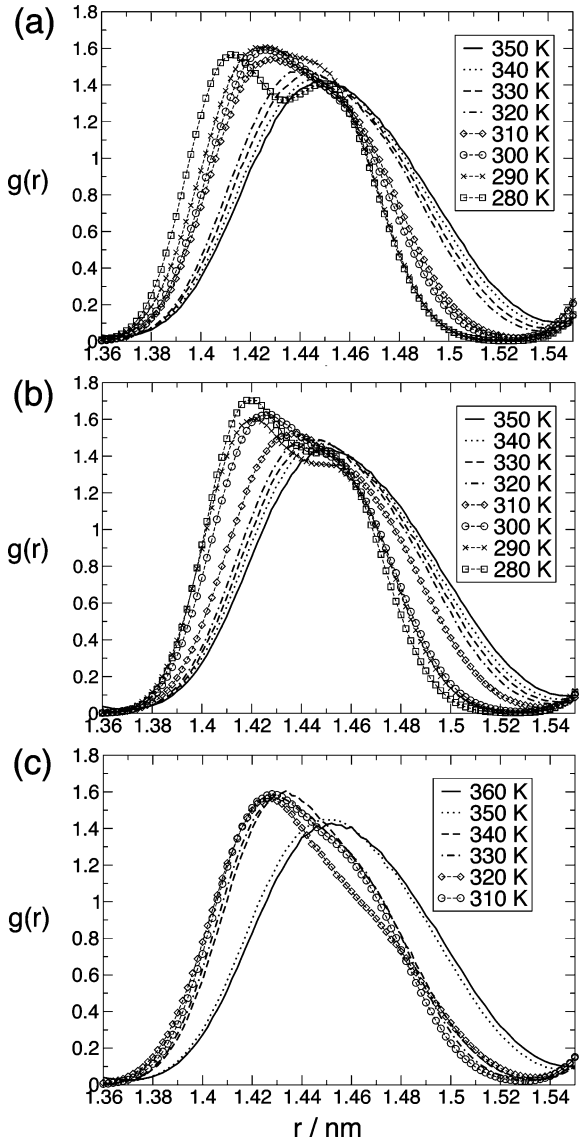

Figure 13. Pair distribution function (PDF) between 1.36 and 1.55 nm, corresponding to the fourth coordination sphere, calculated for the three isomers (a) *o*-carborane, (b) *m*-carborane, and (c) *p*-carborane at various temperatures in the molecular dynamics simulation.

amplitude increases, indicating less vibrational and librational motion as the system cools. All the different coordination spheres show at least two different regions as a function of the simulation temperature, with the boundaries occurring at about 315, 310, and 345 K for *o*-, *m*-, and *p*-carborane, respectively. For all three isomers, the distributions appear to become bimodal at low temperatures, with this being most noticeable for *o*-carborane; although the effect is slight, it is tempting to interpret this as corresponding to the reduction in crystal symmetry observed in some diffraction studies of the low-temperature phases.

To understand the molecular motion of each isomer, we have calculated the rotational correlation function for the CH and BH bonds at different simulation temperatures. Figure 14 shows the values for τ_c for the three isomers. In each case, a biexponential fit to the correlation function was used and two different values of τ_c were obtained, which we describe as the high-frequency (short τ_c) and low-frequency (long τ_c)

DOI: 10.1021/acs.jpcb.5b00043
J. Phys. Chem. B 2015, 119, 4309−4320

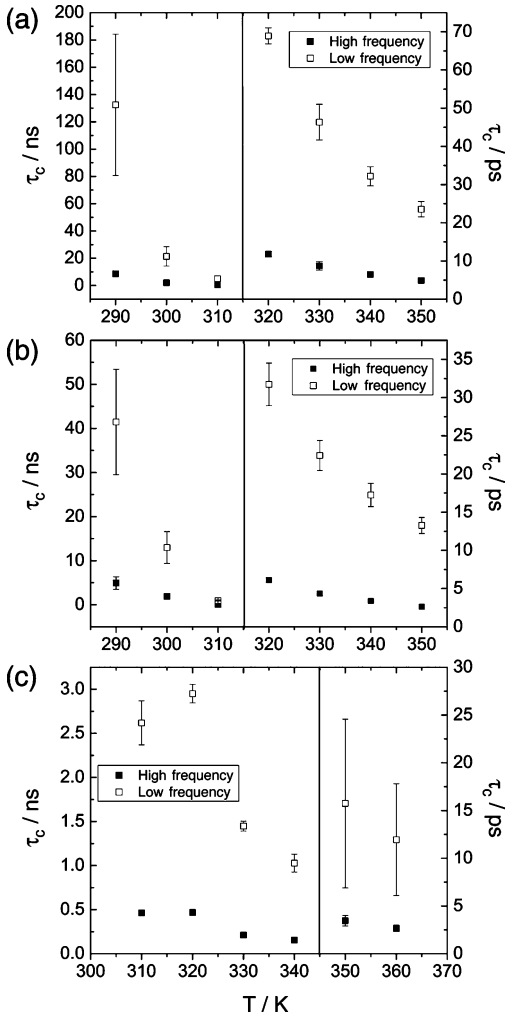

Figure 14. Rotational correlation times τ_c for the CH and BH bonds at different temperatures in the molecular dynamics simulations for the three isomers (a) *o*-carborane, (b) *m*-carborane, and (c) *p*-carborane. In each case, a biexponential fit to the correlation function was used, and two different values of τ_c were obtained, which we describe as the high-frequency (short τ_c) and low-frequency (long τ_c) components. The vertical bars span the range of τ_c values found in the molecule: a large vertical bar thus indicates a high degree of anisotropy in the molecular tumbling. The scale on the right-hand side is in picoseconds (ps) and on the left is in nanoseconds (ns); the vertical line in each graph indicates where the scale switches.

components. The vertical bars span the range of τ_c values found in the molecule: a large vertical bar thus indicates a high degree of anisotropy in the molecular tumbling. At high temperatures, the values of τ_c are in the picosecond range; at low temperatures, they are in the nanosecond range. For *p*-carborane at higher temperatures, the values of τ_c for the CH bonds are larger than for the BH bonds. Furthermore, at low temperatures, it was impossible to calculate a correlation time for the CH bond; the correlation function was not an exponential decay, and so we believe that τ_c is longer than the duration of our trajectory. These observations confirm that the molecular rotation for *p*-carborane is predominantly around the C_5 axis of molecular symmetry. For *o*- and *m*-carborane, at higher temperatures the tumbling is more similar for each CH or BH bond (the vertical bars are smaller than for *p*-carborane), but we still find two components for the correlation function and hence two τ_c values. In general, the molecular tumbling observed in *o*-carborane is slower than in *m*-carborane, especially at low temperatures, while both of these isomers exhibit slower tumbling than *p*-carborane, again especially at low temperatures.

From the values of τ_c and *ab initio* values of the ^{11}B quadrupolar coupling constants, the ^{11}B quadrupolar spin–lattice relaxation time was calculated using Bloembergen–Purcell–Pound theory.[26] The Fourier transform of the correlation function with a biexponential decay provided the spectral density.[27] The theoretical values of T_1 are compared with the experimentally determined values in Figure 15 for *o*- and *m*-carborane. Note that we have used the same T_1 scale for both theoretical and experimental values but that we kept different theoretical and experimental temperature scales, empirically aligning the two at the phase transition temperature. It can be seen that, although the theoretical T_1 values tend to underestimate the experimental ones in the high-temperature phase, that the trends in the two sets of values are remarkably similar.

4. CONCLUSIONS

The experimental NMR results presented here show that high-resolution MAS and multiple-quantum MAS spectroscopy are valuable techniques for studying plastic solids containing quadrupolar nuclei. The icosahedral carborane isomers showed

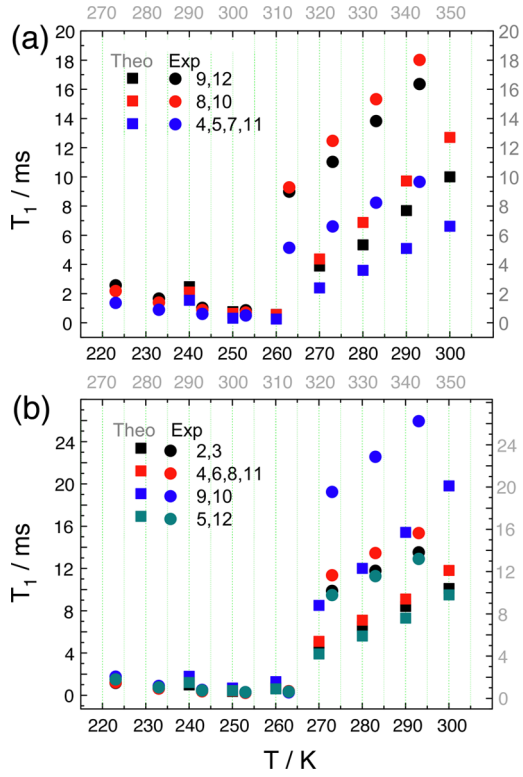

Figure 15. Theoretical ^{11}B spin–lattice relaxation times for (a) *o*-carborane and (b) *m*-carborane calculated using Bloembergen–Purcell–Pound theory for quadrupolar relaxation. The assignment of the symbols refers to the numbering scheme for the boron atoms and peaks in Figures 2 and 3. The Fourier transform of the biexponential correlation functions provided by the molecular dynamics simulations yielded the spectral densities. The experimental ^{11}B spin–lattice relaxation times are shown on the same scale, but we have empirically aligned the experimental and molecular dynamics temperature scales at the phase transition.

DOI: 10.1021/acs.jpcb.5b00043
J. Phys. Chem. B 2015, 119, 4309–4320

liquid-like spectra in phase I, consistent with the earlier work of Harris et al.[4] Below the I–II phase transition, the peaks broaden and spinning sidebands appear, consistent with anisotropic tumbling. By inspecting spinning sideband and MQMAS spectra, it was possible to semiquantitatively probe the nature of tumbling in the three carborane isomers.

Molecular dynamics simulations reveal a structure for all three isomers that is based on a face-centered cubic unit cell. At low temperatures the molecules are essentially static, exhibiting only very rapid librational motions. However, at higher temperatures, two distinct regimes of molecular motion are found where the molecules undergo much larger reorientational jumps. In one of these regimes (the one at lower temperatures), the reorientation is on the nanosecond time scale and appears to be predominantly about a preferred axis (anisotropic motion), whereas in the other regime (at higher temperatures) the correlation time is on the picosecond time scale and the motion appears to be essentially fully isotropic. These molecular dynamics results appear to be in qualitative agreement with the NMR results, including the ^{11}B T_1 measurements.

The change in the reorientational dynamics in the simulations can be attributed to a change in the nonbonding energies when the phase transition occurs. The intermolecular distance between *closo*-carborane molecules decreases with decreasing temperature until it reaches a point where the molecules start to interact strongly with each other, decreasing the rate of molecular reorientation.

The experimental P_Q^{eff} values as a function of temperature are in agreement with the behavior observed in the molecular dynamics simulations, where the dynamic shift can be related directly with the molecular rotation. The molecular motion of *p*-carborane is around the molecular C_5 axis of symmetry at low temperature. This is reflected in P_Q^{eff} falling steadily almost to zero as the temperature is increased. For *o*- and *m*-carborane the motion at high temperature is highly isotropic.

Using ^{11}B MAS NMR and molecular dynamics, we have been able to gain new insight into the dynamic behavior of the *closo*-carboranes. In particular, the molecular dynamics simulations provide strong support for the experimental results, although the phase-transition temperatures are overestimated by at least 30 K in the simulations.

AUTHOR INFORMATION

Corresponding Author

*E-mail: stephen.wimperis@glasgow.ac.uk (S.W.).

Author Contributions

H.A. and T.K. contributed equally to this work.

Notes

The authors declare no competing financial interest.

ACKNOWLEDGMENTS

We are grateful to Becas Chile for a postdoctoral fellowship (H.A.) and to EPSRC for support (Grant GR/T23824). We also thank Professor Alan Welch (Heriot-Watt) for supplying the carboranes and Dr. Hans Senn (Glasgow) for access to the computer cluster facilities.

REFERENCES

(1) Köster, R.; Grassberger, M. A. Structures and Syntheses of Carboranes. *Angew. Chem., Int. Ed.* **1967**, *6*, 218–240.

(2) Baughman, R. H. NMR Calorimetric and Diffraction Study of Molecular Motion in Crystalline Carboranes. *J. Chem. Phys.* **1970**, *53*, 3781–3789.

(3) Beckmann, P.; Leffler, A. J. Solid State Phase Transitions and Molecular Reorientation in Ortho- and Para-Carborane: An Isomer Effect. *J. Chem. Phys.* **1980**, *72*, 4600–4607.

(4) Harris, R. K.; Bowles, J.; Stephenson, I. R.; Wong, E. H. High-Resolution Solid-State ^{11}B and ^{13}C MAS NMR of Icosahedral Carboranes. *Spectrochim. Acta, Part A* **1988**, *44*, 273–276.

(5) Reynhardt, E. C.; Froneman, S. Phase Transitions and Molecular Motions in Crystalline Ortho- and Meta-Carborane. *Mol. Phys.* **1991**, *74*, 61–78.

(6) Leites, L. A. Vibrational Spectroscopy of Carboranes and Parent Boranes and Its Capabilities in Carborane Chemistry. *Chem. Rev.* **1992**, 279–323.

(7) Diogo, H. P.; Correia, N. T.; Moura Ramos, J. J. Phase Transitions and Phase Transformations in Crystalline Ortho- and Meta-Carboranes. *J. Phys. Chem. Solids* **2005**, *66*, 832–838.

(8) Winterlich, M.; Böhmer, R.; Diezemann, G.; Zimmermann, H. Rotational Motion in the Molecular Crystals Meta- and Ortho-Carborane Studied by Deuteron Nuclear Magnetic Resonance. *J. Chem. Phys.* **2005**, *123*, 094504.

(9) Frydman, L.; Harwood, J. S. Isotropic Spectra of Half-Integer Quadrupolar Spins from Bidimensional Magic-Angle Spinning NMR. *J. Am. Chem. Soc.* **1995**, *117*, 5367–5368.

(10) Poupko, R.; Baram, A.; Luz, Z. Dynamic Frequency Shift in the ESR Spectra of Transition Metal Ions. *Mol. Phys.* **1975**, *27*, 1345–1357.

(11) Werbelow, L. G. NMR Dynamic Frequency Shifts and the Quadrupolar Interaction. *J. Chem. Phys.* **1979**, *70*, 5381.

(12) Westlund, P. O.; Wennerström, H. NMR Lineshapes of $I = 5/2$ and $I = 7/2$ Nuclei. Chemical Exchange Effects and Dynamic Shifts. *J. Magn. Reson.* **1982**, *50*, 451–466.

(13) Werbelow, L.; London, R. E. Dynamic Frequency Shift. *Concepts Magn. Reson.* **1996**, *8*, 325–338.

(14) Gamba, Z.; Powell, B. M. The Condensed Phases of Carboranes. *J. Chem. Phys.* **1996**, *105*, 2436–2440.

(15) Kurkiewicz, T.; Thrippleton, M. J.; Wimperis, S. Second-Order Quadrupolar Shifts as an NMR Probe of Fast Molecular-Scale Dynamics in Solids. *Chem. Phys. Lett.* **2009**, *467*, 412–416.

(16) Hess, B.; Kutzner, K.; Van der Spoel, D.; Lindahl, E. GROMACS 4: Algorithms for Highly Efficient, Load-Balanced, and Scalable Molecular Simulation. *J. Chem. Theory Comput.* **2008**, *4*, 435–447.

(17) Humphrey, W.; Dalke, A.; Schulten, K. VMD: Visual Molecular Dynamics. *J. Mol. Graphics* **1996**, *14*, 33–38.

(18) Berendsen, H. J. C.; Postma, J. P. M.; van Gunsteren, W. F.; Dinola, A.; Haak, J. R. Molecular Dynamics with Coupling to an External Bath. *J. Chem. Phys.* **1984**, *81*, 3684–3690.

(19) Darden, T.; York, D.; Pedersen, L. Particle Mesh Ewald: An Nlog(N) Method for Ewald Sums in Large Systems. *J. Chem. Phys.* **1993**, *98*, 10089–10092.

(20) Essmann, U.; Perera, L.; Berkowitz, M. L. The Origin of the Hydration Interaction of Lipid Bilayers from MD Simulation of Dipalmitoylphosphatidylcholine Membranes in Gel and Liquid Crystalline Phases. *Langmuir* **1995**, *11*, 4519–4531.

(21) Ngola, S. M.; Zhang, J.; Mitchell, B. L.; Sundararajan, N. Strategy for Improved Analysis of Peptides by Surface-Enhanced Raman Spectroscopy (SERS) Involving Positively Charged Nanoparticles. *J. Raman Spectrosc.* **2008**, *39*, 611–617.

(22) Timofeeva, T. V.; Suponitsky, K. Y.; Yanovsky, A. I.; Allinger, N. L. The MM3 Force-Field for 12-Vertex Boranes and Carboranes. *J. Organomet. Chem.* **1997**, *536*, 481–488.

(23) Lötz, A.; Voitländer, J. The Nuclear Quadrupole Coupling of ^{10}B and ^{11}B in the Carboranes $B_{10}C_2H_{12}$. *J. Chem. Phys.* **1991**, *95*, 3208–3212.

(24) Cutajar, M.; Ashbrook, S. E.; Wimperis, S. ^{2}H Double-Quantum MAS NMR Spectroscopy as a Probe of Dynamics on the Microsecond Timescale in Solids. *Chem. Phys. Lett.* **2006**, *423*, 276–281.

DOI: 10.1021/acs.jpcb.5b00043
J. Phys. Chem. B 2015, 119, 4309–4320

(25) Thrippleton, M. J.; Cutajar, M.; Wimperis, S. Magic Angle Spinning (MAS) NMR Linewidths in the Presence of Solid-State Dynamics. *Chem. Phys. Lett.* **2008**, *452*, 233−238.
(26) Jaccard, G.; Wimperis, S.; Bodenhausen, G. Multiple-Quantum NMR Spectroscopy of $S = 3/2$ Spins in Isotropic Phase: A New Probe for Multiexponential Relaxation. *J. Chem. Phys.* **1986**, *85*, 6282−6293.
(27) Mauzac, M.; Vairon, J. P.; Lauprêtre, F. Nuclear Spin-Lattice Relaxation and Molecular Motions in Isotactic Poly(But-1-ene) and (But-1-ene)-Propylene Copolymers in Solution. *Polymer* **1979**, *20*, 443−449.

DOI: 10.1021/acs.jpcb.5b00043
J. Phys. Chem. B 2015, 119, 4309−4320